Formulation and characterization of a biocompatible microemulsion composed of mixed surfactants: lecithin and Triton X-100

Arindam Das · Rajib Kumar Mitra

Abstract We report on the formation and characterization of a biocompatible microemulsion (ME) system composed of lecithin (L), Triton X-100 (T) as the surfactant(s), butyl lactate (BL) as the cosurfactant, and isopropyl myristate (IPM) as the oil phase and water. Detailed phase construction reveals that mixing of surfactants (L and T) produces larger single-phase ME region compared to L. In the mixed surfactant systems, a three-phase body appears which is otherwise not obtained in the single surfactant counterparts signifying the synergistic solubilization behaviour upon mixing. The maximum solubilization capacity decreases as the content of T increases in the mixture. Viscosity, conductance and adiabatic compressibility measurements of the single-phase ME systems at a constant amphiphile concentration (80 % *w*/*w*) show a linear trend with increasing water content revealing a droplet-type structure of all the studied formulations. FTIR studies in the water-in-oil (w/o) region identify the presence of three distinct types of water molecules in these systems and their relative content changes with the interfacial composition as well as the total water content in the system. Our study offers a biocompatible mixed ME system in which the physical properties do not differ much from those of the lecithin-based systems with the additional advantage of having higher solubilization capacity, low pH dependency and low viscosity, which renders its potential to be used for specific pharmaceutical applications.

A. Das · R. K. Mitra (✉)
Department of Chemical Biological and Macromolecular Sciences, S.N. Bose National Centre for Basic Sciences, Block JD, Sector III, Salt Lake, Kolkata 700098, India
e-mail: rajib@bose.res.in

Keywords Lecithin · Triton X-100 · Mixed microemulsion · Three phase · Solubilization capacity · Viscosity · Conductivity · FTIR

Introduction

Microemulsions (ME) are isotropic, fluid, transparent, thermodynamically stable dispersion of oil and water, stabilized by surfactant(s) [1, 2]. The structure of ME can be idealized as a set of interfaces dividing polar and nonpolar domains. Depending on the composition of the system, the microstructure of an ME may exist as water-in-oil (w/o) droplets, oil-in-water (o/w) droplets, or a bicontinuous structure. Over the last few decades, MEs have attracted more interest as potential drug delivery systems [3–5]. Part of this interest appears as a consequence of their transparency, ease of preparation, nanometric size and long-term stability. These properties as well as their ability for incorporating drugs of different lipophilicity are some of the reasons for which MEs have seriously been considered for pharmaceutical purposes. However, the limitations on the use of MEs in pharmaceutical and cosmetic fields arise greatly from the need for all the constituting components to be biologically and pharmaceutically acceptable, particularly the surfactants and cosurfactants. The selection of components for MEs suitable for cosmetic and pharmaceutical use is one of the most important factors to fulfil the requirements of a good delivery system. One of the most preferred biocompatible ME is based on lecithin (L), which is a nontoxic surfactant as recognized by safe (GRAS) status[6]. Being highly lipophilic, lecithin tends to form nematic liquid crystalline phases in the presence of oil and water [5]. Biocompatible lecithin-based organogels have been found to be clear and viscoelastic and are used for pharmaceutical applications [7]. Phase behaviour, structure and pharmaceutical applications of lecithin/short-chain alcohol-based ME

systems have also been investigated in details [8–16]. Low toxic formulation has been reported using linker molecules [17–19]. Many of these formulations, however, possess high viscosity, which refrains these formulations from specific pharmaceutics applications. Moreover, the short-chain alcohols used in the ME systems are prone to affect cell membrane [20]. It thus stands important to formulate low-toxicity, low-viscosity ME systems containing lecithin and cosurfactant. A potential replacement of toxic short-chain alkanols is butyl lactate (BL) which is a well-known pharmaceutical flavouring agent [21] and has been used to formulate MEs [22–24].

Mixtures of surfactants have often been found to be advantageous over the use of single surfactants, since they can extract properties superior than the individual ones. Blending of two nonionic surfactants [25] or ionic and nonionic surfactants [26, 27] can provide better solubilization capacity and affect the phase behaviour relative to the individual ones. Blending of surfactants can tune the hydrophilic–lipophilic balance (HLB) of the constituting surfactants in order to optimize the solubilization capacity. Earlier, our group has reported on the phase behaviour as well as other physical properties of a series of mixed ME systems [28–31]. Herein, we report on the detailed phase behaviour and structural aspects of a mixed surfactant ME system composed of lecithin and Triton X-100. TX-100 is a biocompatible [32] and one of the most widely used nonionic surfactants for lysing cells to extract protein and other cellular organelles or to permeabilize the living cell membrane for transfection [33, 34]. We chose isopropyl myristate (IPM) as the oil phase as it has widely been used in biocompatible formulations [14, 15, 23]. The principal objective of this work is to establish the enrichment of solubilization behaviour of this mixed system as a lipophilic surfactant lecithin (HLB~4) is mixed with a hydrophilic surfactant TX-100 (HLB~13.5) to tune the optimum HLB of the mixed system using BL as the cosurfactant. Phase diagrams for the single and mixed surfactant systems have been constructed in order to compare the solubilization behaviour of these systems. The fluidity of these ME systems have been estimated using viscosity measurements. The network structure of water in the oil-rich region is determined by monitoring the O–H stretching frequency modes by FTIR spectroscopy.

Materials and methods

Chemicals (Scheme 1) were obtained from the following sources: lecithin (L), isopropyl myristate (IPM), butyl lactate (BL) and Triton X-100 [polyethylene glycol *p*-(1,1,3,3-tetramethylbutyl)-phenyl ether] (T) were from Sigma Aldrich, and sodium chloride was from Merck. All the chemicals were of the highest commercially available purity and used without further purification. Double-distilled water was used throughout the experiments. Construction of triangular [28] and fishtail [29] phase diagrams can be followed from our earlier studies, and we have studied on these phase diagram at room temperature (~25 °C). In all the triangular phase diagrams, the total surfactant/cosurfactant ratio had been fixed to 1:2 (*w*/*w*). Triangular phase diagram ascertains the limit of single-phase ME domain, whereas fishtail diagrams were constructed to determine the minimum amount of amphiphile required to form single-phase ME. Different phases were identified with visual inspection. The appearance of three-phase region could clearly be identified as the phases are distinct. A representative photograph containing the different phases is shown in Fig. S1 (supporting information section). Appearance of viscous and gel phases were also estimated by visual inspection of the relative motion of the fluid mixture through the walls of the test tubes. All the physical properties were measured using single-phase ME systems of various composition with fixed surfactant/cosurfactant ratio of 1:2 (*w*/*w*).

Viscosity of the ME systems at different temperatures were measured by an automated micro-viscometer (AVMn) from Anton Paar (Austria). High-precision density and sound velocity were measured by a density meter, model DSA-5000 from Anton Paar (Austria), with an accuracy of 5×10^{-6} g cm^3 and 0.5 m s^{-1} in density and sound velocity measurements, respectively.

Electrical conductivity of the ME systems was measured using a SensION378 conductivity meter (Hach Company, Loveland, CO) at room temperature. Since the MEs were based on nonionic components and there is no considerable dependence of phase behaviour on salinity, a solution of 0.9 % NaCl was used as the aqueous phase. Measurement of conductivity was carried out with an absolute accuracy up to ±0.5 %. Adiabatic compressibility (β) of the mixture can be determined by measuring the solution density (ρ) and the sound velocity (u) and applying the Laplace equation,

$$\beta = \frac{1}{\rho u^2} \tag{1}$$

FTIR spectra in the 3,000–3,800-cm^{-1} window were recorded on a JASCO FTIR-6300 spectrometer (transmission mode) using CaF_2 window. It is important to note that IPM has negligible absorbance in this studied frequency range; however, BL has a particular absorbance peak in this region (data not shown). So, the data of BL has been subtracted from the ME systems in order to obtain contribution from water only. We report on the difference absorbance spectra, which are the differences between the measured absorbance of the mixture of (L or T or LT)/BL/IPM systems from the corresponding hydrated ME solutions. Therefore, the difference spectra can be attributed to the water molecules present in the ME systems only.

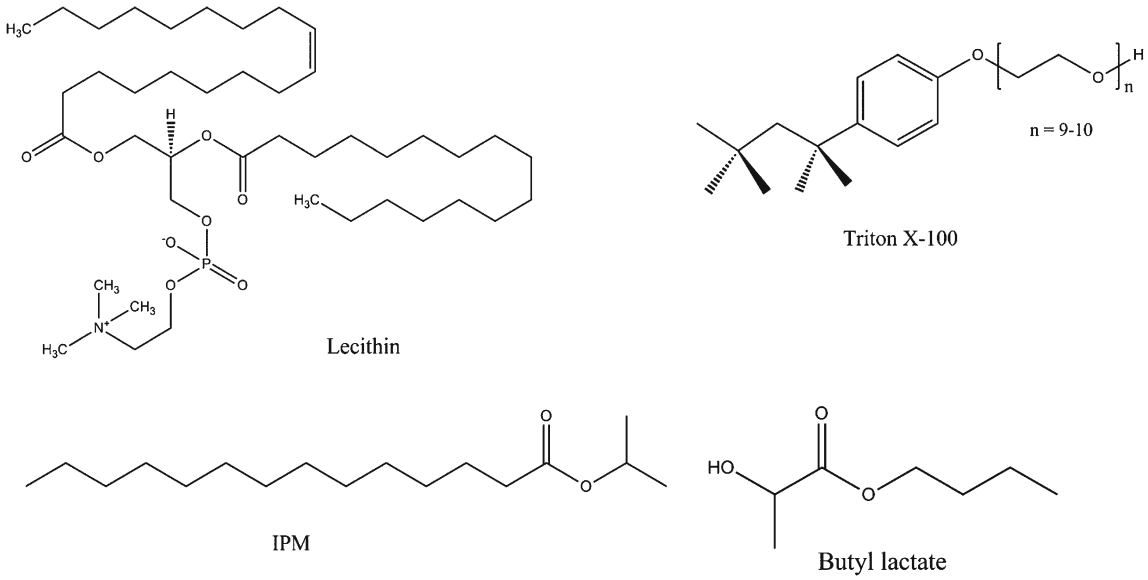

Scheme 1 Molecular structures of lecithin, TX-100, IPM and butyl lactate

Results and discussion

Figure 1a shows the pseudo-ternary phase diagrams of the system composed of L/BL/IPM/water, TX-100/BL/IPM/water and L + TX-100 (1:1, *w*/*w*)/BL/IPM/water at room temperature. We denote these systems as L, T and LT, respectively. The surfactant(s)/BL ratio is kept fixed at 1:2 (*w*/*w*). In the figure, only single-phase ME region has been demarcated. As can be observed from the figure, the system L offers a very thin single-phase region along the amphiphile/oil axis. The system T offers a somewhat larger single-phase region compared to L, expanding in the amphiphile/water axis also. The mixed (LT) system offers even better single-phase region compared to the individual (L and T) systems, especially along the amphiphile/oil axis. The detailed phase diagrams of L and LT are shown in Fig. 1b.

The phase behaviour of L is characteristic of the presence of various meso-phases [19]. It can be observed that there remains a considerable fraction of viscous and gel phases, especially in the oil-rich region. The mixed system, however, offers a less complicated behaviour with the absence of highly viscous or gel phases; rather, a three-phase region appears at low amphiphile concentration. Appearance of a three-phase region signifies a perfect balance of the HLB of the mixed system [35]. This corresponds to a proper mixing of hydrophilic TX-100 and lipophilic lecithin with BL, which brings about enhanced solubilization capacity of the mixed surfactant systems, and thus, a larger ME region is obtained. The single-phase boundary does not appreciably change in the temperature range of 10–40 °C (data not shown). For potential pharmaceutical application, the ME system should also be stable at various physiologically relevant environments, and, to check that, we determine the phase behaviour of the LT system at pH=2.6 and in 0.9 % salt concentration. It is found that the phase behaviour of the LT system remains almost unaltered in these two conditions, revealing the stability of the system in these environments. The pseudo-ternary phase triangle provides with the information on the extent of single-phase

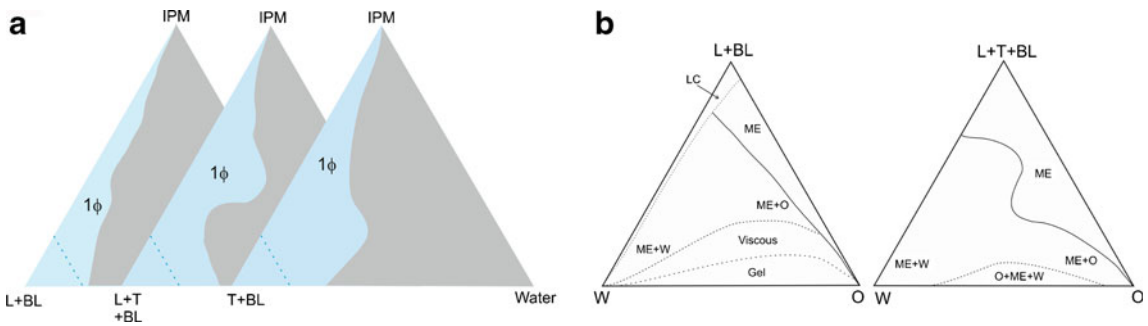

Fig. 1 **a** Pseudo-ternary phase diagrams of lecithin (L)/TX-100 (T)/butyl lactate (BL)/IPM/water systems. The *dotted lines* represent the dilution line through which samples are chosen for physical measurements. The surfactant(s)/cosurfactant ratio is fixed at 1:2 (*w*/*w*). *1φ* represents single-phase ME region. **b** Detailed phase diagram of L and L + T (mixed) systems. The surfactant(s)/cosurfactant ratio is fixed at 1:2 (*w*/*w*). *W*, *O*, *ME* and *LC* represent water, oil (IPM), microemulsion and liquid crystalline phases, respectively

region, and from that, one can choose suitable composition to carry out further physical investigations. Here, we adopt an oil/water dilution route in which the total amphiphile concentration is kept fixed at 80 % in all the three systems. This helps to extract information on the relative change of properties as the dispersed medium changes from oil-rich to water-rich at a fixed amphiphile concentration. We choose five such compositions, in which the oil/water (w/w) ratios are 10:1 (LT1), 2.3:1 (LT2), 1:1 (LT3), 1:2.3 (LT4) and 1:7 (LT5).

In order to extract information on the maximum solubilization capacity, we construct the so-called 'fishtail' diagrams [2]. Vertical sections bisecting the water–oil axis of the phase prism for the pseudo-four-component systems are shown in Fig. 2a in which X stands for the total amphiphile weight fraction: $\left(X = \frac{S+\mathrm{BL}}{O+W+S+\mathrm{BL}}\right)$, where O and W stand for oil and water, respectively; S stands for surfactant(s) (L or T or L + T). W_1 denotes the BL weight fraction in the total amphiphile, i.e. $W_1 = \frac{\mathrm{BL}}{S+\mathrm{BL}}$. In the figure, W III and W IV represent Winsor III (three-phase) and Winsor IV (single-phase) systems, respectively [36]. The appearances of liquid crystal or viscous-gel phase are not shown in the figure. We choose four different compositions depending upon the L/T mixing ratios (w/w), namely, 2:1 (L_2T), 1:1 (LT), 1:2 (LT_2) and 0:1 (T). As can be observed from the figure, three-phase body is observed only in case of LT and LT_2 systems, and not for the other two systems, wherein only single-phase and biphasic bodies are identified. The L system does not produce any single-phase region within the experimental window. Optimum mixture of LT with BL gives rise to a balance ME as manifested with the appearance of a three-phase body as evidenced in LT and LT_2 systems. It is interesting to note that the formation of single-phase domain shifts towards higher X values as the content of T increases in the mixture. We plot the volume fraction of different phases as a function of X (Fig. 2b, inset) in order to understand the composition of the dispersed phases. At high X, the formulation is found to be of W II type (i.e. w/o type ME on top and the excess water phase at the bottom) at a fixed W_1 value. As the amphiphile concentration (X) decreases, the bending elasticity of the interface monolayer changes gradually, and eventually, it tends to bend in an opposite direction to produce W I (Winsor I) systems (o/w ME in the lower phase with excess oil in the upper one) passing through a W III or W IV body. At low W_1, the system is predominantly hydrophilic, and the amphiphile monolayer bends itself around the oil phase in order to produce o/w droplets (W I system). With increasing BL content, the radius of curvature increases, and the droplet nature of the ME is converted into a bicontinuous one, and a Winsor III system is formed. On further increase of BL, the increasing lipophilicity of the amphiphile mixture tunes the monolayer to bend around water in order to produce w/o droplets in oil continuous medium (Winsor II system). The point at which the three-phase body meets the single-phase body corresponds to the maximum solubilization capacity of the system [35], and the corresponding amphiphile concentration is denoted by X_b and that of BL is denoted by $W_{1\mathrm{b}}$. X_b indicates the minimum concentration of total amphiphile (surfactant plus cosurfactant) required for the formation of single-phase microemulsion with equal amount of water and IPM. The lower the value of X_b, the higher is the solubilization capacity. For the present systems, we obtain the X_b and $W_{1\mathrm{b}}$ values to be 0.2, 0.633 for LT and 0.289, 0.65 for the LT_2 systems, respectively. It therefore clearly indicates that the mixed systems exhibit better solubilization behaviour than the corresponding single surfactant systems.

Interfacial composition inside the three-phase body can be estimated in the following manner: for a particular surfactant mixture, the three-phase region is a nonvariant region as all the intensive variables (temperature, pressure and oil–water ratio) are fixed for the pseudo-four-component system. The

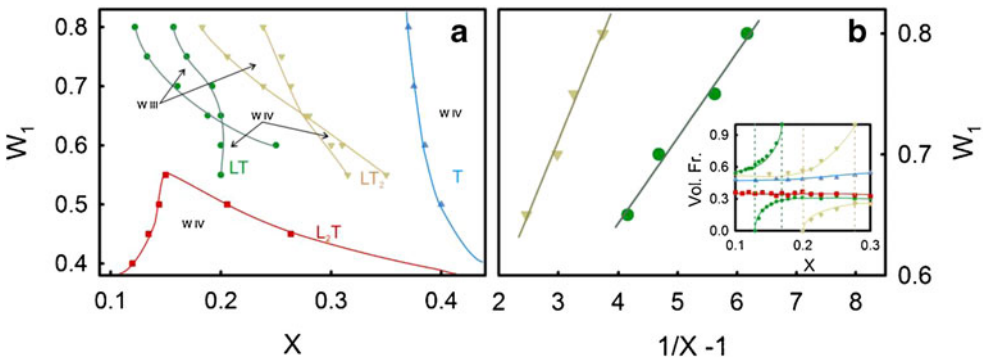

Fig. 2 **a** Vertical sections through the pseudo-quaternary phase prism for lecithin/TX-100/butyl lactate/IPM/water systems at a constant water/oil ratio of 1:1 (w/w). The lecithin/TX-100 ratio has been chosen as follows: 2:1 (L_2T, *red square*), 1:1 (LT, *green circle*), 1:2 (LT_2, *yellow inverted triangle*) and 0:1 (T, *blue triangle*). *W III* and *W IV* stand for tri-phasic and single-phase region, respectively. **b** Butyl lactate weight fraction values (W_1) as a function of ($1/X-1$) obtained from the midpoints of the three-phase bodies in **a**. The *straight lines* are linear fits. The correlation of coefficient (R-squared) values obtained is 0.988 for LT and 0.987 for LT_2 systems, respectively. Volume fraction of the different phases of the systems—L_2T, *red square*; *LT*, *green circle*; LT_2, *yellow inverted triangle*; and *T*, *blue triangle*—for W_1=0.75 are shown in the *inset*. The *dotted lines* enclose three-phase areas

composition and structure of the ME phase along the midst curve in the three-phase body would also be fixed and would essentially be equal to that of the single-phase body at this point [35, 37]. The three-phase region consists of micro-oil and micro-water subdomains separated by amphiphile interface [38]. The surfactant molecules are essentially adsorbed at the micro-oil–water interface and form an interfacial layer. We assume negligible monomeric solubility of the amphiphiles in the micro-oil–micro-water domains. It can be noted here that the total phase behaviour of the pseudo-four-component system can be represented by a composition tetrahedron (in which the four different components act as the vertices of the three-dimensional tetrahedron) at constant temperature and pressure. In such a tetrahedron, an HLB plane [39] of maximum solubilization can be drawn which essentially includes the particular three-phase tie-triangle including the ME in the middle curve of the Winsor III region. The subsequent HLB plane equation is given as follows:

$$W_1 = S_1^S - \frac{S_1\left(1-S_1^S\right)}{\left(1-S_1\right)} \cdot \alpha \cdot \left(\frac{1}{X} - 1\right) \tag{2}$$

where α is the weight fraction of oil in oil and water mixture (herein 0.5), and S_1^S represents the BL solubility in the total amphiphilic mixture (L + T + BL) at the water–oil interface inside the ME phase. S_1 is the monomeric solubility of BL in the micro-oil domain and is equal to the BL fraction in the excess oil phase. S_1^S can be obtained as the intercept of the linear plot of $(1/X-1)$ against W_1, and S_1 can be calculated from the slope of the straight line. We plot $1/X$ as a function of W_1 for the LT and LT_2 systems, and good linear fits are obtained (Fig. 2b). The calculated S_1^S and S_1 values are 0.361 and 0.181 for the LT system, and 0.351 and 0.27 for the LT_2 system, respectively. It appears therefore that in LT system, BL is more localized at the oil–water interface rendering its better solubilization behaviour compared to LT_2. The corresponding surfactant and cosurfactant concentration at the micro-interface can be obtained as follows [29, 40]:

$$C_1 = X_b W_{1b} - \frac{\alpha(1-X_b)}{1-S_1} S_1 \tag{3}$$

$$C_2 = X_b(1-W_{1b}) \tag{4}$$

where C_1 and C_2 are the respective weight fractions of BL and (L + T) in the system at the water–oil interface within the single ME phase at the maximum solubilization point. We calculate the C_1 and C_2 values of 0.04 and 0.075 for the LT system and 0.056 and 0.101 for the LT_2 system, respectively. The rationale behind the observed increase in the solubilization capacity for the 1:1 LT mixture is twofold: firstly, a decreased value of S_1 signifies the lower monomeric solubility of BL in the micro-oil phase which eventually increases the net solubilization capacity of the surfactant layer at the oil–water interface inside the ME, and secondly, a low value of the $C_1 + C_2$ signifies a more efficient interface inside the microemulsion. As a combined effect, the solubilizing power per surfactant molecule itself increases as L and T is mixed in 1:1 (w/w) ratio. We also construct the three-phase behaviour of the LT system in the presence of 0.9 % NaCl (data not shown). It has been found that the maximum solubilization limit is achieved at X_b=0.22 and W_{1b}=0.6 with the corresponding S_1^S and S_1 values of 0.406 and 0.17, respectively. The observed marginal change in the amphiphile distribution profile is consistent with previously reported ME systems [29].

The phase study thus establishes the fact that mixing of surfactants offers enhanced solubilization capacity of the mixed surfactant systems compared to the single ones. We now investigate how the physical properties of the ME system change upon mixing L and T. In order to achieve this, we choose the single-phase ME systems at a fixed amphiphile concentration of 80 % (w/w) and varied the water content following the dotted line shown in Fig. 1a. The choice of amphiphile concentration is to ensure that all the three systems (L, T and LT) produce single-phase ME.

Viscosity is one of the most important macroscopic properties of a ME system which specifies its applications, especially in the field of pharmacology [3, 41–43]. Figure 3 depicts the viscosity profile of all the studied systems. In Fig. 3a, specific viscosity is plotted against the weight fraction of water in the formulations. All the systems follow a Newtonian fluidity and offer a lower viscosity than the previously reported lecithin-based ME/organogel systems [15, 16]. It is observed that the T systems are ~23 %, while the LT systems are ~15 % less viscous than the L systems. This result identifies that mixing of surfactants effectively brings down the viscosity of the lecithin-based systems. Viscosity increases as the content of water increases in all the systems. It can be noted here that IPM has a four to five times higher viscosity than water, yet the water-rich region offers a higher viscosity than the oil-rich region, which might due to the stronger interaction between the droplets, a phenomenon much consistent with the previously reported biocompatible ME systems [23, 28]. However, the observed linear trend of the viscosity profile is markedly different from the apprehended bell-shaped trend in which a w/o droplet system gets converted into a o/w droplet system passing through an intermediate bicontinuous phase [28]. The viscosity results thus strongly identify the droplet character of all the chosen samples. The viscosities of all these systems are measured at different temperatures in order to probe the energetic of the viscous flow. Figure 3b depicts the viscosity behaviour of the mixed surfactant systems at different temperatures (20–60 °C). With increase in temperature, viscosity expectedly decreases. The activation enthalpy

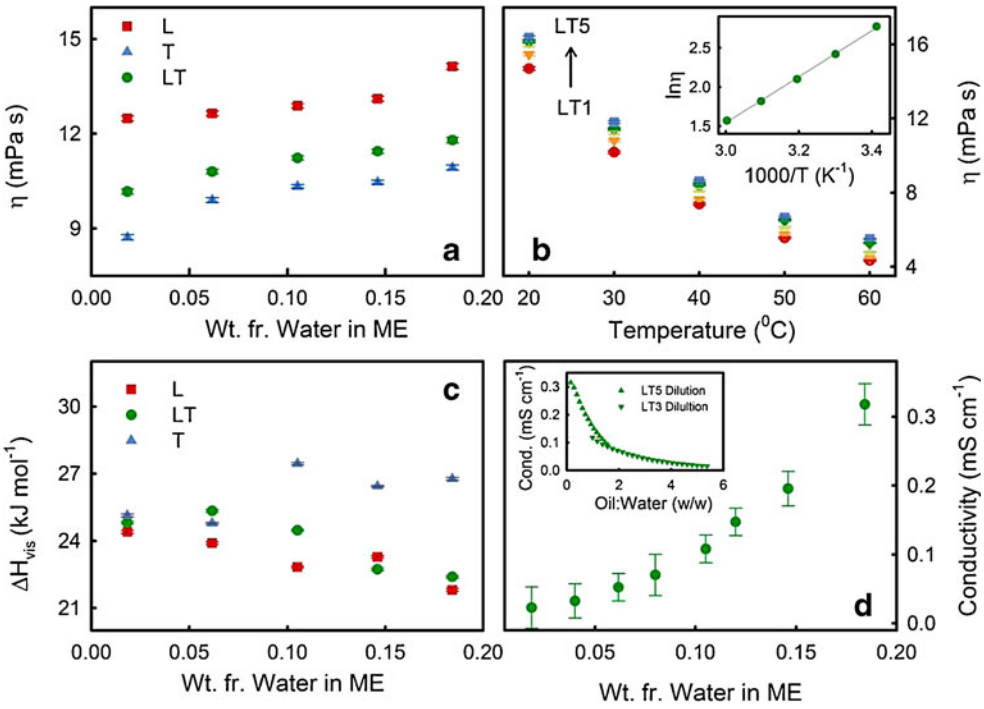

Fig. 3 **a** Viscosity of three different ME systems L, LT and T as a function of water content in the ME. **b** Viscosity of LT ME system as a function of temperature. *Inset*: Plot of ln η vs $1/T$ for a representative LT ME system. The *straight line* corresponds to a linear fit. The correlation of coefficient (R-squared) value is 0.99. **c** The activation enthalpy (ΔH^*_{vis}) of three different ME systems L, LT and T as a function of water content in the ME. **d** Conductivity of LT ME systems as a function of water concentration in ME. *Inset*: Conductivity as a function of oil–water weight ratio for two dilution routes

ΔH^*_{Vis} (which is equivalent to the energy of activation for viscous flow ΔE^*_{Vis}) is obtained from [28] the following:

$$\eta = \frac{Nh}{V}\exp\left(\frac{\Delta H^*_{vis}}{RT}\right)\exp\left(-\frac{\Delta S^*_{vis}}{R}\right) \quad (5)$$

where h is the Plank constant, N is the Avogadro number, V is the molar volume, and ΔS^*_{Vis} is the entropy of activation for the viscous flow; other terms have their usual significance.

Assuming ΔS^*_{Vis} to be independent of temperature, a straight line plot between ln η vs. T^{-1} is expected from the slope of which ΔH^*_{Vis} can be calculated. All the studied systems produce good linear fits for ln η vs T^{-1} plot. A representative plot has been shown in Fig. 3c. The obtained ΔH^*_{Vis} values for all the systems are plotted in Fig. 3c as a function of water content. The values range in the order of 20–25 kJ mol^{-1}, which is in good agreement with other biocompatible ME systems [28]. The ΔH^*_{Vis} values do not follow any significant trend; for L and LT systems, it suffers a marginal decrease, whereas for the TX-100-based system, it shows a slight increase beyond 10 % water content. The absence of any remarkable trend in ΔH^*_{Vis} coupled with the observed linearity in specific viscosity rules out the possibility of the presence of any bicontinuous phase in the chosen concentration regime. We also determine the specific viscosity of the LT systems at two terminal pH conditions of pH=2.0 and 12.0 in order to check their sustainability in drastic physiological conditions. It has been found that viscosity of the LT systems offer only marginal variation (Figs. S2 and S3, supporting information section) indicating their potential to be applied for specific pharmaceutical applications.

The transition of structures in ME systems can also be monitored through conductance studies, which offers detectable change as the dispersing phase changes its polarity. We measure the conductivity of the mixed system (in the presence of 0.9 % NaCl) as a function of water concentration, and the result is depicted in Fig. 3d. It can be observed from the figure that conductivity increases expectedly with increasing water concentration and a distinct change in the slope can unambiguously be identified at 10 % water content, which signifies a sharp transition of the dispersant medium from oil continuous to water continuous. It could be noted here that 10 % water content corresponds to an equal oil–water ratio, and in many systems, such a system offers bicontinuous phase. In a previous study with Tween-80/BL/IPM system, the conductivity profile showed two distinct changes in the slopes identifying a w/o to o/w phase through an intermediate bicontinuous phase [23]. The appearance of a single break in the slope signifies a sharp w/o to o/w droplet transition in the present study as also has been evidenced from the viscosity studies. We also measure the conductivity as a function of oil/water (w/w) ratio following oil dilution lines starting from LT3 (water/amphiphile (w/w)=0.125) and LT5 (water/amphiphile (w/w)=0.23). We observe two distinct slopes intersecting at oil/water=1 (Fig. 3d, inset) strongly corroborating our conclusion of the droplet nature of all the systems.

Figure 4 shows the iso-entropic compressibility β for all the studied systems. β expectedly decreases as the system

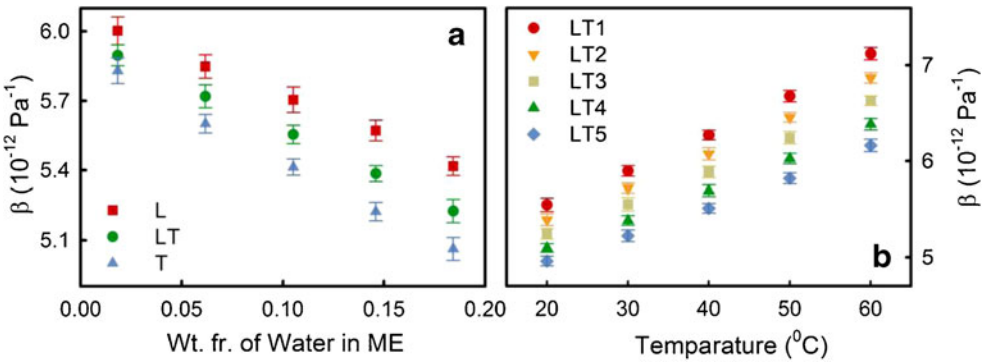

Fig. 4 **a** Compressibility (β) of three different ME systems L, LT and T as a function of water content. **b** Variation of compressibility (β) of different LT systems as a function of temperature

becomes more water rich. The observed higher compressibility of the system at low water content is in good agreement with the viscosity behaviour of the system, which suggests the hard sphere-like character of the water globules in oil-continuous medium (w/o). The temperature dependency of β also shows a linear trend (Fig. 4b), which strongly demands the absence of any intermediate structural modification other than the droplet type.

The equilibrium structural features of different components in self-assembled systems could efficiently be resolved using FTIR spectroscopy. Previously, lecithin-based reverse micellar systems in hydrocarbon oils have been studied using FTIR spectroscopy [44–46]. While much attention has been paid on the P=O and C–H bond stretching vibrations of lecithin molecule, studies on the structural alteration of water is rather sparse [47, 48]. It often stands necessary, especially during the application of w/o type ME as a water-soluble drug carrier, to understand how the equilibrium structure of water modifies with the change in composition. In the present study, we measure the MIR (mid-infrared) FTIR spectra of LT1, LT2 and LT3 systems to determine the water structure inside the ME droplets. From the conductance study (Fig. 3d), LT1 and LT2 systems can safely be assumed to possess w/o type droplets, while LT3 is in the onset of formation of o/w type droplets. In all these measurements, we subtract the data of surfactant (or mixture of surfactants)/BL/IPM ternary systems from the hydrated quaternary systems, and thus, the signals essentially provide information on the water molecules present in the systems only. We focus our attention to the 3,000–3,800-cm^{-1} frequency window as this is a fingerprint region for the symmetric and asymmetric vibrational stretch of O–H bonds in water [49]. A representative FTIR spectrum has been shown in Fig. 5a.

The FTIR spectrum of water in this frequency window can be deconvoluted into three Gaussian sub-bands peaking at ~3,600-, 3,460- and 3,330-cm^{-1} regions [50]. The peak at ~3600 cm^{-1} is due to the 'multimer' or 'bound type' water molecules which make bonds with the interface and thus do not produce strong hydrogen bonds with the neighbouring water molecules and have generally been realized in extreme hydrophobic environments. The second component peaking at 3,460 cm^{-1} involves the so-called 'intermediate' water molecules which are unable to develop fully hydrogen bonds and somewhat connected to other water molecules with distorted H bonds. Finally, the third kind of water molecule (i.e. peaking at 3,330 cm^{-1}) originates from the 'network' or 'bulk type' water molecules which are fully hydrogen bonded with the neighbouring water molecules and contributes its majority of share in pure water. We deconvolute the MIR spectra of all the systems into three Gaussian components keeping the peak positions fixed as those of pure water (a representative figure is shown in Fig. 5a). A free fitting often produces more accurate contributions; however, fixing the peak positions allows comparing the change in the relative weightage of each component at variable interfacial compositions. We plot the relative contribution of each curve towards the total spectra and plot it as a function weight percentage of water (Fig. 5b–d). This relative contribution is essentially proportional to the fraction of water molecules belonging to that particular stretching mode. In a previous study by Maitra et al. [47] in lecithin-based reverse micellar systems, the FTIR spectra had been deconvoluted into two contributions: one peaking at ~3,250 cm^{-1} (bound water) and the other at ~3,460 cm^{-1} (free water). The relative content of these molecules had been found to be dependent on the system composition. We herein prefer a three-peak fitting, which provided better fitting results compared to the two-peak fittings.

It can be observed from Fig. 5d that the relative abundance of the multimer water molecules decreases with increasing water content, which is due to the formation of strongly hydrogen-bonded water network at elevated water concentration. The lecithin-based system shows a lower abundance of the multimer water molecules compared to the TX-100-based systems, with the LT systems lying in between. It is interesting to note that for the L1, T1 and LT1 systems, where the water concentration is only ~2 %, the difference is very marginal, which perhaps is apprehended taking into account the tight binding nature of water molecules with the interface. The population corresponding to the intermediate water (peaking at 3,460 cm^{-1}) shows marginal variation with water content,

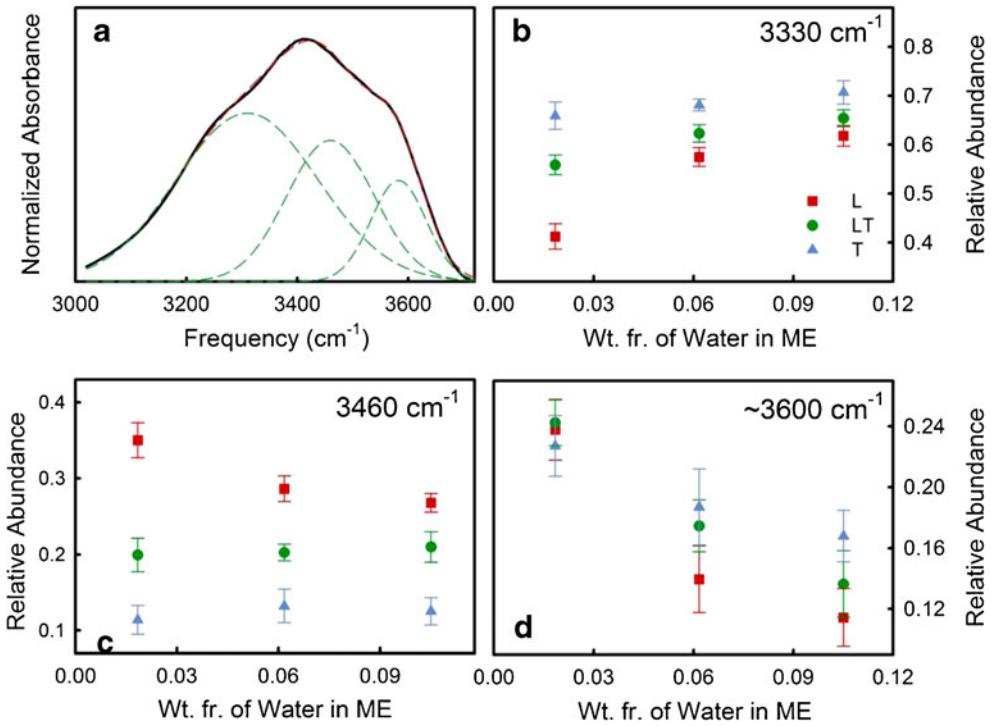

Fig. 5 **a** A representative FTIR curve deconvoluted into three different contributions (*green broken lines*). The *red broken line* represents the overall fit. The relative area under curves peaking at 3,330 cm^{-1} (**b**), 3,460 cm^{-1} (**c**) and ~3,600 cm^{-1} (**d**) for the three different ME systems L, LT and T are shown as a function of water content in the ME

especially for the T and LT systems, with a faint decreasing trend for the corresponding L systems (Fig. 5c). The population of network water (peaking at 3,330 cm^{-1}) increases with increasing the weight percentage of water, faintly with the LT and T systems, and considerably with the L systems (Fig. 5b). As mentioned earlier, the abundance of network water is a signature of the bulk nature of the water present in the systems. In pure water, this corresponds to ~70 %. As observed from the figure, such abundance is eventually reached for the T-based system, while for the LT system, it increases from 55 % (for the w/o system) to 64 % (for o/w system), and for L, it increases from 40 to 61 %. This shows that in L-based systems, the water structure is more perturbed than the corresponding T and LT systems. Interestingly, L also has the lowest abundance of the multimer water, confirming a high abundance of intermediate water, which suggests a strong interaction between lecithin and water. Earlier studies by Carvallro et al. [48] concluded insignificant effect of water content on the FTIR spectra, whereas Maitra et al. [47] concluded that the O–H bond stretching frequency suffers significant change upon interaction with lecithin and also depends upon the nature of the oil phase. However, it should be taken into consideration that both these previous studies dealt with visco-elastic reverse micellar systems with very low water content. Our investigated systems are relatively low-viscous ME containing 2–10 % (*w*/*w*) water, which explains the presence of three different species of water molecules and the observed variation in their relative abundance with different interfacial compositions. We carry out the FTIR studies at two terminal pH conditions of pH=2.0 and 12.0 in order to determine whether the water structure suffers any perturbation at different pH conditions. The results are shown in Fig. S4 (supporting information section). It is evident that the relative population of various type of water is independent of the pH of the aqueous phase.

Conclusions

The present investigation was aimed towards the formulation of a lecithin-based biocompatible low-viscous microemulsion system. Most of the previously reported lecithin-based formulations are visco-elastic gel-like formulations [15, 16], and for certain specific applications, it is important to formulate low-viscous systems. Lecithin being highly lipophilic is very sensitive to form gel-like structures; however, blending with a hydrophilic surfactant TX-100 and a lipophilic cosurfactant butyl lactate produces considerable low-viscous microemulsion systems, with a synergistic enhancement of single-phase region compared to the individual surfactants. The mixed systems produce a three-phase body which reveals a perfect hydrophilic–lipophilic balance and maximum solubilization limit, which is otherwise not obtained with either lecithin or TX-100. The increased solubilization capacity is due to the decrease in both S_1 (monomeric solubility of BL in the micro-oil domain) as well as small values of C_1+C_2 (increased effective solubilization capacity of the amphiphiles). Viscosity, conductivity and adiabatic compressibility measurements provide evidences of droplet nature of the formulations at high surfactant concentrations. FTIR

spectroscopic studies in the oil-rich regions identifies the presence of three distinct types of water molecules present in the systems, and the relative abundance of such type of water molecules changes with composition. The measured physical properties of the mixed surfactant systems do not drastically differ from those obtained for the lecithin-based systems and is also independent on pH and the presence of electrolytes with the additional advantage of being less viscous. Our study thus offers a biocompatible low-viscous lecithin-based ME system that can serve as a basis for further investigations in drug delivery and as nontoxic nanotemplates for other applications in the future.

Acknowledgments AD acknowledges UGC, Government of India, for a research fellowship. RKM acknowledges CSIR, India for a research grant (no. 01(2573)/12/EMR-II), Unit for Nano Science and Technology, and Theme Unit of Excellence on Nano-device Technology at S.N. Bose Centre for support.

References

1. Paul BK, Moulik SP (1997) Microemulsions: an overview. J Disp Sci Technol 18:301–367
2. Kahlweit M (1988) Microemulsions. Science 240:617–621
3. Kogan A, Garti N (2006) Microemulsions as transdermal drug delivery vehicles. Adv Colloid Interf Sci 123–126:369–385
4. Lawrence MJ, Rees GD (2012) Microemulsion-based media as novel drug delivery systems. Adv Drug Deliv Rev 64:175–193
5. Tenjarla S (1999) Microemulsions: an overview and pharmaceutical applications. Crit Rev Ther Drug Carrier Syst 16:461–521
6. Acosta EJ, Nguyen T, Witthayapanyanon A, Harwell JH, David DA, Sabatini A (2005) Linker-based bio-compatible microemulsions. Environ Sci Technol 39:1275–1282
7. Raut S, Bhadoriya SS, Uplanchiwar V, Mishra V, Gahane A, Jain SK (2012) Lecithin organogel: a unique micellar system for the delivery of bioactive agents in the treatment of skin aging. Acta Pharm Sin B 2:8–15
8. von Corswant C, Thorén PEG (1999) Solubilization of sparingly soluble active compounds in lecithin-based microemulsions: influence on phase behavior and microstructure. Langmuir 15:3710–3717
9. Wolf G, Kleinpeter E (2005) Pulsed field gradient NMR study of anomalous diffusion in a lecithin-based microemulsion. Langmuir 21:6742–6752
10. Papadimitriou V, Sotiroudis TG, Xenakis A (2007) Olive oil microemulsions: enzymatic activities and structural characteristics. Langmuir 23:2071–2077
11. Tzika ED, Christoforou M, Pispas S, Zervou M, Papadimitriou V, Sotiroudis TG, Leontidis E, Xenakis A (2011) Influence of nanoreactor environment and substrate location on the activity of horseradish peroxidase in olive oil based water-in-oil microemulsions. Langmuir 27:2692–2700
12. Harms M, Mackeben S, Müller-Goymann CC (2005) Thermotropic transition structures in the ternary system lecithin/isopropyl myristate/water. Colloids Surf A Physicochem Eng Asp 259:81–87
13. Pestana KC, Formariz TP, Franzini CM, Sarmento VHV, Chiavacci LA, Scarpa MV, Egito EST, Oliveira AG (2008) Oil-in-water lecithin-based microemulsions as a potential delivery system for amphotericin B. Colloids Surf B: Biointerfaces 66:253–259
14. Changez M, Varshney M, Chander J, Dinda AK (2006) Effect of the composition of lecithin/*n*-propanol/isopropyl myristate/water microemulsions on barrier properties of mice skin for transdermal permeation of tetracaine hydrochloride: In vitro. Colloids Surf B: Biointerfaces 50:18–25
15. Brime B, Moreno MA, Frutos G, Ballesteros MP, Frutos P (2002) Amphotericin B in oil–water lecithin-based microemulsions: formulation and toxicity evaluation. J Pharm Sci 91:1178–1185
16. Moreno MA, Ballesteros MP, Frutos P (2003) Lecithin-based oil-in-water microemulsions for parenteral use: pseudoternary phase diagrams, characterization and toxicity studies. J Pharm Sci 92:1428–1437
17. Yuan JS, Ansari M, Samaan M, Acosta EJ (2008) Linker-based lecithin microemulsions for transdermal delivery of lidocaine. Int J Pharm 349:130–143
18. Yuan JS, Acosta EJ (2009) Extended release of lidocaine from linker-based lecithin microemulsions. Int J Pharm 368:63–71
19. Xuan XY, Cheng YL, Acosta E (2012) Lecithin-linker microemulsion gelatin gels for extended drug delivery. Pharmaceutics 4:104–129
20. McKarns SC, Hansch C, Caldwell WS, Morgan WT, Moore SK, Doolittle DJ (1997) Correlation between hydrophobicity of short-chain aliphatic alcohols and their ability to alter plasma membrane integrity. Fundam Appl Toxicol 36:62–70
21. Rowe RC, Sheskey PJ, Owen SC (2006) Handbook of pharmaceutical excipients, 5th edn. Pharmaceutical Press and American Pharmacists Association, London
22. Comelles F, Pascual A (1996) Microemulsions with butyl lactate as cosurfactant. J Disp Sci Technol 18:161–175
23. Saha R, Rakshit S, Mitra RK, Pal SK (2012) Microstructure, morphology, and ultrafast dynamics of a novel edible microemulsion. Langmuir 28:8309–8317
24. Mitra RK, Paul BK (2003) Physicochemical studies on mixed surfactant microemulsion systems iii. Phase behaviours of microemulsions derived from a nonionic surfactant (Brij-56) and the influence of ionic surfactants, cosurfactants, oil, temperature and additives. J Surf Sci Technol 19:139–158
25. Kunieda H, Yamagata M (1993) Mixing of nonionic surfactants at water–oil interfaces in microemulsions. Langmuir 9:3345–3351
26. Kahlweit M, Faulhaber B, Busse G (1994) Microemulsions with mixtures of nonionic and ionic amphiphiles. Langmuir 10:2528–2532
27. Silas JA, Kaler EW, Hill RM (2001) Effect of didodecyldimethylammonium bromide on the phase behavior of nonionic surfactant–silicone oil microemulsions. Langmuir 17:4534–4539
28. Mitra RK, Paul BK (2005) Physicochemical investigations of microemulsification of eucalyptus oil and water using mixed surfactants (AOT + Brij-35) and butanol. J Colloid Interface Sci 283:565–577
29. Mitra RK, Paul BK (2005) Effect of temperature and salt on the phase behavior of nonionic-ionic microemulsions with fish-tail diagram. J Colloid Interf Sci 291:550–559
30. Mitra RK, Paul BK (2006) Physicochemical investigations of (anionic-nonionic) mixed surfactant microemulsions in non-aqueous polar solvents: I phase behavior. Colloid Polym Sci 284:733–744
31. Nandy D, Mitra RK, Paul BK (2006) Phase behavior of the mixtures of polyoxyethylene(10) stearyl ether (Brij-76), 1-butanol, isooctane and mixed polar solvents: water and formamide (or *N*, *N*-dimethyl formamide). J Colloid Interface Sci 300:361–367
32. Ostroumov SA (2005) Biological effects of surfactants. CRC, Boca Raton
33. Gennuso F, Fernetti C, Tirolo C, Testa N, L'Episcopo F, Caniglia S, Morale MC, Ostrow JD, Pascolo L, Tiribelli C, Marchetti B (2004) Bilirubin protects astrocytes from its own toxicity by inducing up-regulation and translocation of multidrug resistance-associated protein 1 (Mrp1). Proc Natl Acad Sci U S A 101:2470–2475
34. Rajagopal A, Pant AC, Simon SM, Chen Y (2002) In vivo analysis of human multidrug resistance protein (MRP1) activity using transient expression of fluorescently tagged MRP1. Cancer Res 62:391–396

35. Kunieda H, Nakano A, Pes MA (1995) Effect of oil on the solubilization in microemulsion systems including nonionic surfactant mixtures. Langmuir 11:3302–3306
36. Winsor PA (1948) Hydrotropy, solubilisation and related emulsification processes. Trans Faraday Soc 44:376–398
37. Pes MA, Aramaki K, Nakamura N, Kunieda H (1996) Temperature-insensitive microemulsions in a sucrose monoalkanoate system. J Colloid Interface Sci 178:666–672
38. Pes MA, Kunieda H (1995) Surfactant distribution in mixed surfactant microemulsions. Trends Phys Chem 5:75–89
39. Kunieda H, Shinoda K (1985) Evaluation of the hydrophile-lipophile balance (HLB) of nonionic surfactants. I. Multisurfactant systems. J Colloid Interface Sci 107:107–121
40. Li X, Ueda K, Kunieda H (1999) Solubilization and phase behavior of microemulsions with mixed anionic–cationic surfactants and hexanol. Langmuir 15:7973–7979
41. Garti N (2003) Microemulsions as microreactors for food applications. Curr Opin Colloid Interf Sci 8:197–211
42. Garti N, Yaghmur A, Leser ME, Clement V, Watzke HJ (2001) Improved oil solubilization in oil/water food grade microemulsions in the presence of polyols and ethanol. J Agric Food Chem 49:2552–2562
43. Garti N, Yaghmur A, Aserin A, Spernath A, Elfakess R, Ezrahi S (2003) Solubilization of active molecules in microemulsions for improved environmental protection. Colloids Surf A Physicochem Eng Asp 230:183–190
44. Shervani Z, Jain TK, Maitra A (1991) Nonconventional lecithin gels in hydrocarbon oils. Colloid Polym Sci 269:720–726
45. Arcoleo V, Goffredi M, La Manna G, Turco Liveri VT, Aliotta F (1997) Study of lecithin reverse micelles by FT-IR spectroscopy. Prog Colloid Polym Sci 105:220–223
46. Ruggirello A, Liveri VT (2003) FT-IR investigation of the urea state in lecithin and sodium bis(2-ethylhexyl)phosphate reversed micelles. J Colloid Interface Sci 258:123–129
47. Maitra A, Jain TK, Shervani Z (1990) Interfacial water structure in lecithin-oil–water reverse micelles. Colloids Surf 47: 255–267
48. Carvallaro G, La Manna G, Liveri VT, Aliotta F, Fontanella ME (1995) Structural investigation of water/lecithin/cyclohexane microemulsions by FT-IR spectroscopy. J Colloid Interface Sci 176: 281–285
49. Corcelli SA, Skinner JL (2005) Infrared and Raman line shapes of dilute HOD in liquid H2O and D2O from 10 to 90 °C. J Phys Chem A 109:6154–6165
50. Das A, Patra A, Mitra RK (2013) Do the physical properties of water in mixed reverse micelles follow a synergistic effect: a spectroscopic investigation. J Phys Chem B 117:3593–3602